Water Science & Technology

IWA PUBLISHING

Water Science & Technology Vol 85 No 4, 1053 doi: 10.2166/wst.2022.024

Evaluation of process condition impact on copper and lead ions removal from water using goethite incorporated nanocomposite ultrafiltration adsorptive membranes

Seyedeh-Soghra Hossaini-Zahed[a], Samaneh Khanlari[a,b], Omid Bakhtiari[c,†], Maryam Ahmadzadeh Tofighy[a,†], Soheil Hadadpour[a], Saeid Rajabzadeh[d], Pengfei Zhang[d], Hideto Matsuyama[d] and Toraj Mohammadi[a,*]

[a] Centre of Excellency for Membrane Science and Technology, Department of Chemical, Petroleum and Gas Engineering, Iran University of Science and Technology (IUST), Narmak, Tehran, Iran
[b] Department of Chemical Engineering, McMaster University, Hamilton, Ontario L8S 4L7, Canada
[c] Membrane Research Center, Faculty of Petroleum and Chemical Engineering, Razi University, Kermanshah, Iran
[d] Research Center for Membrane and Film Technology, Department of Chemical Science and Engineering, Kobe University, Rokkodaicho 1-1, Nada, Kobe 657-8501, Japan
*Corresponding author. E-mail: torajmohammadi@iust.ac.ir
†Both authors had an equal contribution.

SR, 0000-0003-2883-4587; TM, 0000-0003-0455-3254

ABSTRACT

Polyacrylonitrile (PAN) adsorptive membrane incorporated with nanosize-goethite (α-FeO(OH)) hydrous metal oxide particles (GNPs), prepared with optimal flux and Cu(II) removal in the previous study, was used to evaluate the process parameter on the Cu(II) removal. Box-Behnken Design (BBD) based on the Response Surface Methodology (RSM) was employed to evaluate the impact of Cu(II) feed solution characteristics such as pH, initial concentration of metal ion, and transmembrane pressure (TMP) on copper removal efficiency. The outcomes indicated that the RSM optimization technique could be utilized as an applicable method to find the optimum condition for the maximum Cu(II) removal with slight variance compared with the experimentally measured data. The effect of each process parameter and the coupling effect of parameters on the Cu(II) removal was assessed. Finally, the optimum condition of pH, Cu(II) concentration, and transmembrane pressure (TMP) to obtain high copper removal efficiency was decided. In the optimum condition of the Cu(II) removal, the removal of lead (Pb(II)) metal ion was evaluated by the same membrane.

Key words: Box-Behnken experimental design, goethite nanoparticle, metal ion removal, nanocomposite adsorptive membrane, water treatment

HIGHLIGHTS

- Systematic investigation on the membrane operating condition variables.
- Optimization of the operation condition using response surface methodology.
- Promoted membrane separation performance with incorporation of goethite nanoparticles.
- High membrane flux for heavy metal removal from wastewater using adsorptive membranes.

GRAPHICAL ABSTRACT

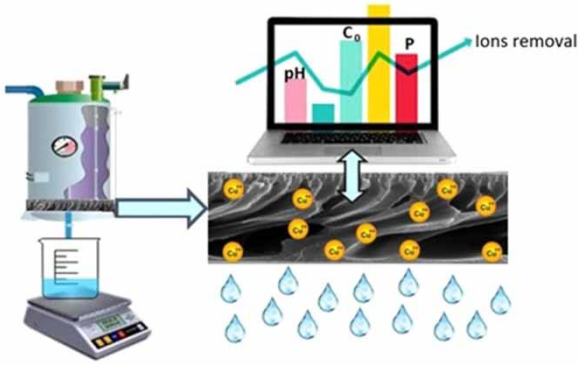

INTRODUCTION

In the previous few decades, a remarkable quantity of hazardous wastes has been imposed on the human and wild environment as a result of urbanization and industrialization. Especially, the fast increasing heavy metal ions in rivers, surficial streams and wastewaters must be considered as a major life threatening preoccupation (Cao *et al.* 2010). Unlike organic pollutants, metal ions are not degradable and produce a hazard of accumulation in humans' organs. Moreover, they are potential risks for the environment, plants, animals, and marine life, especially at higher dosages (Tofighy & Mohammadi 2011). All aforementioned concerns, along with the increasing shortage of freshwaters and competitive use of existing water resources, have made heavy metal ion removal from water more important than it was before. Chemical precipitation (Charerntanyarak 1999), ion exchange (Lalmi *et al.* 2018), adsorption (Faur-Brasquet *et al.* 2002), coagulation (Charerntanyarak 1999) and flocculation (Hankins *et al.* 2006), flotation (Deliyanni *et al.* 2017), electrochemical treatment (Tran *et al.* 2017) and membrane filtration (Borbély & Nagy 2009) are different methods developed to remove metallic ions from effluents, among which membrane technology is one of the most frequently studied methods according to literature surveys (Fu & Wang 2011). Therefore, membrane-based ion removal techniques experienced a highly noticeable growth toward resolving or diminishing problems associated with metal ions present in water streams and wastewaters. Numerous metal ions were targeted for these endeavours, such as copper (Cu^{2+}) (Ghaemi 2016; Hossaini Zahed *et al.* 2019), mercury (Hg^{2+}), zinc (Zn^{2+}) (Borbély & Nagy 2009), lead (Pb^{2+}) (Rahimi *et al.* 2015), cadmium (Cd^{2+}) (Choi & Kim 2003), nickel (Ni^{2+}) (Ho *et al.* 2014), and cobalt (Co^{2+}) (Verbeken *et al.* 2009) ions, which are detected in industrial effluents.

Nanocomposite membranes are a new generation of membranes that are fabricated by incorporating nanomaterials with polymeric membrane materials. Incorporating nanomaterials affects membrane performance in two different ways. First, it alters polymeric membrane characteristics such as hydrophilicity, porosity, electric charge density and mechanical stability, and second, it introduces unique functionalities such as antibacterial, photocatalytic or adsorptive capabilities (Yin & Deng 2015). Usually, nanomaterials are included to overcome the demerits of the typical membranes, such as passing over the trade-off between rejection and water permeability, avoiding membrane fouling, and increasing membrane thermal and chemical stability. In case the added nanomaterials would be hydrophilic, segregation of the added nanoparticles from the bulk of the membrane to the surface of the membrane increased the hydrophilicity and increased the surface pore size, porosity and water permeability due to the faster phase separation rate (Mulder 1997). In a high concentration of nanomaterials, dope solution viscosity increases, which delays mixing and decreases the pore size, porosity, and water permeability of the resultant membrane.

In Hossaini Zahed *et al.* (2019), goethite nanoparticles (GNPs) were incorporated into a polyacrylonitrile (PAN)-based UF membrane, and the fabricated membranes were investigated to remove Cu(II) ion from synthesized wastewater. An effective membrane-based ion removal efficiency can be obtained by optimizing the membrane fabrication condition and the process parameter optimization, feed pH, initial concentration, and transmembrane pressure (TMP) to remove the targeted pollutant from wastewater. In this paper, only the effects of the membrane fabrication conditions were investigated, and the impacts of the process conditions were not yet evaluated.

Feed pH is known as an effective parameter in many separation processes. Song and Htun (Oo & Song 2009) found that feed pH plays a crucial role in boron ion removal in a reverse osmosis membrane. They concluded that higher feed pH values result in greater boron ion removal. This is due to the dissociation of boric acid into borate form, and there exists a significant repulsion force between the membrane surface and borate charges at higher pH values. In another study, the effect of feed solution pH was investigated in some membrane-based processes such as separation of albumin from immunoglobulins (Saksena & Zydney 1994) and separation of oil via ultrafiltration (UF) of oil/water/nonionic surfactant emulsion (Fazullin & Mavrin 2017). To the best of our knowledge, no study has yet focused on the effect of feed pH on ion removal efficiency in effluent treatment using adsorptive nanocomposite membranes.

Different effluents contain different amounts of metal ion contaminants according to different processes. Thus, initial feed metal ion concentration is another important factor. However, different researchers have studied to find the optimum concentration at which the highest ion removal is achieved. For example, Ahmad *et al.* studied the effect of contaminant copper and lead ion concentration on the efficiency of the removal process (Sani *et al.* 2017). Omri and Benzina also conducted a study to evaluate the effect of feed contaminant concentration on removal efficiency and found that at a fixed pH, the lower ion concentration typically results in better removal efficiency (Omri & Benzina 2012). However, to the best of our knowledge, no experimental evaluation has been performed at a variety of pH ranges.

TMP is a crucial factor affecting the separation performance of the membrane-based separation for the removal of organic and inorganic species. Mnif *et al.* (2015) studied the effect of TMP on phenol removal from water in reverse osmosis filtration and concluded that higher TMP leads to higher phenol removal. Arsenic semi-metallic ion removal from wastewaters was studied at several TMPs using four commercial nanofiltration (NF) membranes by Zhao *et al.* (Yu *et al.* 2013). Similarly, they concluded that more ions are removed as a result of higher TMP. However, few studies have focused on the effect of TMP on ion removal performance of low-pressure filtration like UF. Although Huang *et al.* (2012) assessed the effect of TMP on membrane fouling in separating Cd^{2+} ion from contaminated synthetic wastewater, the authors mainly focused on the membrane fouling, and decrease in membrane water permeability and the effect of TMP on the ion removal efficiency were not evaluated (Huang *et al.* 2012).

In the previous published paper (Hossaini Zahed *et al.* 2019), only the effect of membrane fabrication condition on the divalent metal ion was evaluated, and the impact of process conditions was not assessed. Although some studies have performed a preliminary evaluation of the process conditions on the metal ion removal from the water, these phenomena were not evaluated well. Therefore, this study focused on the effect of the change in feed solution and process operating conditions on removal efficiency. In other words, for a UF nanocomposite membrane embedded with GNPs, feed initial ion concentration and pH were studied, and their mutual effects were considered for the first time. Moreover, operational optimum TMP was chosen based on the preliminary screening tests. To the best of our knowledge, the effect of the process conditions on the nanocomposite UF membrane has been rarely studied. Thus, the effect of process parameters was focused on in this study.

EXPERIMENTAL

Materials

Iron nitrate nonahydrate ($(FeNO_3)_3.9H_2O$, 99% purity), as a precursor for nanoparticles synthesis, cupric nitrate ($Cu(NO_3)_2$, 98% purity), hydrochloric acid (HCl, 37% purity), sodium and potassium hydroxide (NaOH, >98% purity, and KOH, >85% purity), poly(vinylpyrrolidone) (PVP, 10 kg mol^{-1}), as pore former, and dimethylacetamide (DMAc, 99% purity), as a solvent, were purchased from Merck™. Lead nitrate ($Pb(NO_3)_2$, 99% purity) was supplied from Fluka™. Polyacrylonitrile (PAN, 350 kg mol^{-1}), as membrane polymer matrix, and all other chemicals were purchased from domestic chemical suppliers. All the polymers and the synthesised GNPs were dried (1 h at 70 °C) in a vacuum oven prior to being used.

Nanoparticles synthesis

Goethite, as a kind of ferrous hydroxide (α-FeO(OH)) with the hydroxyl-covered surface, was added to the polymeric matrix to improve its hydrophilicity and consequently the obtained membrane performance in water-based separations (Rahimi *et al.* 2015). The synthesis of goethite briefly involves hydrolysis of the ferric salts in their aqueous solutions, refinement, and finally, separation of the products, as first introduced in 2003 by Bakoyannakis *et al.* (2003) as a simple and cost-effective method. In order to synthesize GNPs, some minor changes were applied accordingly. Initially, 4.85 g of $Fe(NO_3)_3.9H_2O$ was dissolved in 50 mL of distilled deionized water, and the solution was then precipitated by the gradual addition of 4.8 M KOH solution while it was subjected to highly fast stirring conditions until the solution basic pH of 12 was attained. Then the suspension was sonicated with the power of 305 W at ambient temperature for 30 min and then placed in an oven for 70 min at 100 °C before centrifugation for 10 min at 10,000 rpm. Finally, the achieved solid nanoparticles were washed with acetone and distilled deionized water, and last of all, dried at ambient temperature (Rahimi *et al.* 2015).

Nanocomposite membrane fabrication

This study selected the phase separation method for membrane fabrication due to its versatility and simplicity. Hence, GNPs were first dispersed in sufficient DMAc utilizing the maximum power of an ultrasound probe for 15 min. PAN and PVP were gradually added to the suspension within 6 h, at 50 °C while it was stirring at 200 rpm. PAN and PVP powders were already kept in an oven at 70 °C overnight in order to remove any potential adsorbed humidity. After all, the mixture was kept stirred for 30 h at 100 rpm. At this point, the mixture of PAN/PVP/GNPs/DMAc was completely homogeneous and set for casting. A casting knife (thickness = 200 μm) was then used to cast the mixture at ambient temperature, and then it was submerged in distilled water for a whole day prior to being tested as the membrane. Membrane composition in this study was 15 wt. % of PAN, 1.3 wt. % of PVP, 0.1 wt. % of GNPs, and the rest up to 100% was DMAc (83.6 wt. %). More detailed information about membrane preparation is available in our previously published paper (Hossaini Zahed *et al.* 2019). Based on the previous

study (Hossaini Zahed *et al.* 2019), this is the composition at which UF nanocomposite adsorptive membrane showed the optimum water flux of 258 liters per square meter per hour (LMH)/bar and Cu(II) removal of 49.1%. Membrane without nanoparticle inclusion was also prepared to assess the effect of nanoparticle incorporation.

Membrane characterization

A scanning electron microscope (SEM) was employed to study the morphology of the membranes prepared in this study. Cross-sectional specimens were made by immediately breaking the membrane samples right a few seconds after their immersion in liquid nitrogen. Then the specimens were fixed on fixtures and gold-coated to the thickness of 10 nm, using a C7620 mini Sputter Coater ™ (United Kingdom) prior to being evaluated using a TESCAN™ SEM VEGA.

Transmission electron microscopy (TEM) images were recorded from ultrathin specimens with a thickness of 80 nm, using a M/s Leica diamond knife (Germany) equipped Leica EM UC7 ultra-microtome. TEM images were recorded at an accelerating voltage of 100 kV on a Zeiss-EM10C instrument (Germany).

Experimental design

According to some preliminary screening tests, the feed solution concentration and pH and the operating TMP were recognized as the most important affecting parameters. Accordingly, the feed solution pH (ranged from 2 to 5), Cu(II) concentration (C_0) (ranged from 20 to 200 ppm), and TMP (varied from 1 to 3 bar) were selected as the affecting independent parameters according to the results of the preliminary test and then some new experiments were designed for further evaluation using experimental design method. Table 1 lists the selected affective parameters/levels chosen for the response surface methodology (RSM). Membrane Cu(II) removal results were analysed by means of RSM – Box-Behnken design (BBD) mode (Hossaini Zahed *et al.* 2019; Peng *et al.* 2020; Singh & Bhateria 2020).

Membrane performance measurement

The membrane feed solution was formed by the addition of predetermined amounts of cupric nitrate ($Cu(NO_3)_2$) to a sufficient amount of distilled water at room temperature under the medium speed of agitation. The feed solution pH with predetermined Cu(II) concentration was adjusted by dropwise addition of 0.1 M HCl solution. A sufficient amount of distilled water was then added to the solution to make it meet the designed concentration.

Removal of ions was assessed by means of a dead-end membrane setup using membrane samples with an operative surface of 10.2 cm^2. The cast membranes were located in the cell and subjected to pre-compaction via running pure water for 10 min at a pressure of 3 bar prior to being tested during the real test to remove the compaction effect. Figure 1 depicts a schematic representation of the membrane setup used in this study.

The ion removal performance of the membranes (R) was calculated using Equation (1):

$$R\ (\%) = 1 - C_{ip}/C_{if} \tag{1}$$

where C_{ip} and C_{if} reflect Cu(II) or Pb (II) ion concentrations in permeate and feed solutions (mol m^{-3} or any arbitrary unit), respectively, which was measured using conductivity meter, HANNA instrument (HI2300 EC/TDS/pH meter, Romania). The metal concentration was evaluated by measured conductivity using the calibration curve. To ensure reproducibility of the obtained results, all the examinations were done three times using different membrane samples, and their means were reported as the desired response. All experiments in this study were repeated three times, and only average values were reported. The maximum standard deviation of the results was 7% for ion removal.

Table 1 | Selected important variables and their levels for experimental evaluation of Cu(II) removal using nanocomposite membranes

		Level		
Factor	**Number**	**Low**	**Middle**	**High**
pH	X_1	2	3.5	5
C_0 (ppm)	X_2	20	110	200
TMP (bar)	X_3	1	2	3

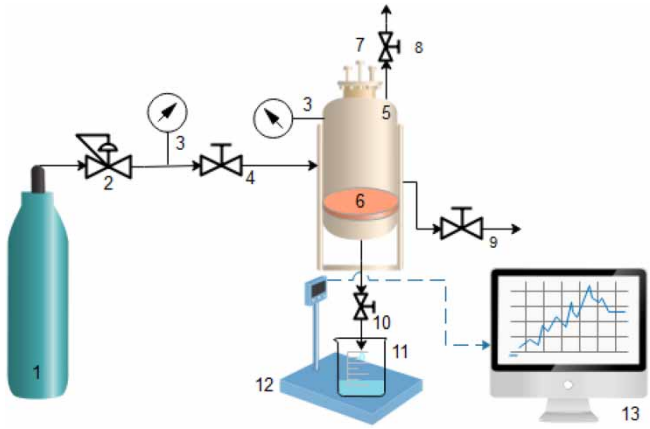

Figure 1 | Schematic representative of the employed dead-end membrane setup: (1) N_2 cylinder, (2) gas regulator, (3) pressure gauge, (4) N_2 pressurizing valve, (5) membrane cell, (6) membrane, (7) feed solution entrance, (8) N_2 vent value, (9) drain valve, (10) permeate valve, (11) permeate collection beaker, (12) digital balance and (13) data acquisition system.

RESULTS AND DISCUSSION

Synthesized nanoparticles' properties

Similarly to the results obtained in the previous study (Hossaini Zahed *et al.* 2019), the formation of the GNP clusters and aggregates is completely obvious from the SEM image shown in Figure 2, originating from the magnetic properties of the GNP nanoparticles. Henceforth, it was somewhat challenging to record any SEM image wherein GNP nanoparticles can be observed separately. Nonetheless, their particle size was observed up to 60 nm and could be identified confidently in the nanometric range. Their surface area, average pore volume, and pore size were 200.8 $m^2 g^{-1}$, 0.40 $m^3 g^{-1}$, and 10.6 nm, respectively, using the nitrogen adsorption-desorption method (Micromeritics ASAP 2020, USA) (Hossaini Zahed *et al.* 2019).

Prepared membranes' properties

Figure 3 shows SEM images of the surface and the cross-sectional views of the control and the 0.1 wt. % GNPs loaded nanocomposite membranes. In Figure 3(a), the surface image of the control membrane demonstrates a smooth surface, as usual for control polymeric membranes. However, as shown in Figure 3(b), the observed GNPs on the nanocomposite membrane surface give it a somewhat grainy look. Knowing the hydrophilic property of the GNPs due to their surface hydroxyl groups, they

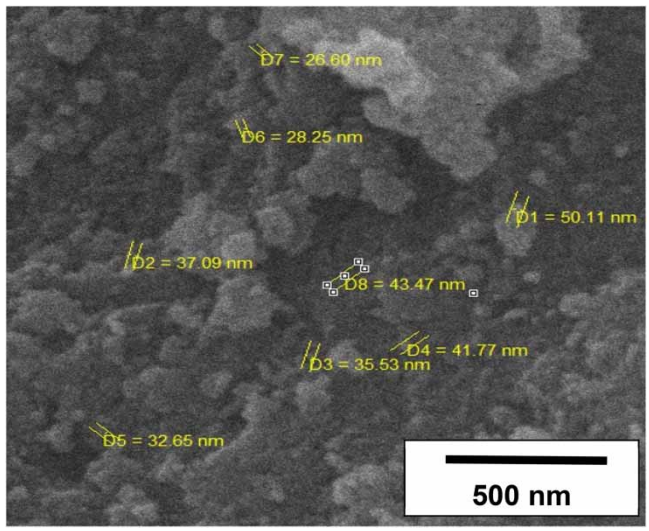

Figure 2 | SEM image of the synthesized GNPs.

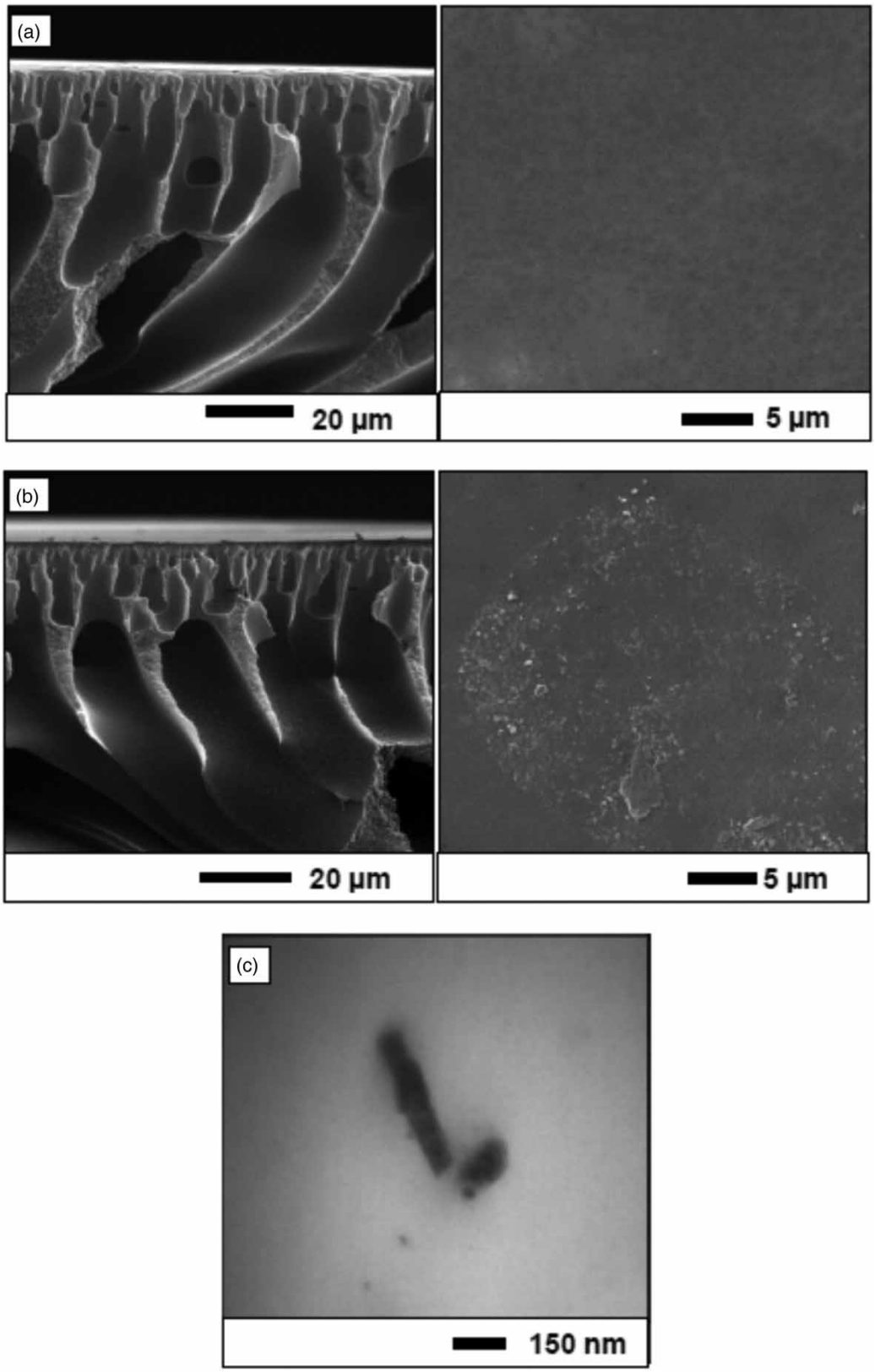

Figure 3 | SEM images of (a) control membrane, (b) nanocomposite membrane (0.1 wt. % GNPs loaded) in which cross-section and surface are left to right-hand, and (c) TEM images of membrane containing 0.1 wt. % GNPs. The surface SEM image of the control PAN membrane was used from Hossaini Zahed *et al.* (2019) with copyright permission from Elsevier.

have the tendency to migrate to the membrane upper surface during phase separation (Chatterjee & De 2014). Although not shown here, in the previous study (Hossaini Zahed *et al.* 2019), the water contact angle of the membrane surface decreased from 67 to 46° by addition of just 0.1 wt. % GNPs, which proves the hypothesis of the GNPs' migration to the membrane surface. The cross-sectional images of both control and nanocomposite membranes show the asymmetric structure, i.e., the porous surface on the top and finger-like structure underneath. This morphology directly results from quick phase separation on the top and rather gentle underneath, as discussed by Bakeri *et al.* in detail (Delavar *et al.* 2017).

Figure 3(c) displays a TEM graph recorded from the cast nanocomposite membrane (0.1 wt.% GNPs). As observed, distinct nano-rods attributed to GNPs were found in the microtomic specimen, demonstrating a proper dispersion of GNPs in the membrane.

Although not shown here, similarly to the previous published paper (Hossaini Zahed *et al.* 2019), Fourier transform infrared (FTIR) revealed proper incorporation of GNPs in the PAN polymer matrix by considering the surface hydroxyl groups in GNPs. The FTIR analysis results can be found in detail in the previous study (Hossaini Zahed *et al.* 2019).

Experimental design on the metal ion removal in the filtration process

In the present research, effects of two feed characteristic factors, namely pH and initial ion concentration, and one operational parameter, i.e. TMP, on the membrane ion removal performance were investigated by carrying out 12 designed experiments based on the BBD method with three replicates to find an inaccuracy in the trials. Table 2 presents the trial plan for the experiments. As presented in the Table, the trials were repeated three times at the center point, namely pH = 3.5, $C_0 = 110$ ppm, and TMP = 2 bar, to compute the error of the model. The last three experiments (rows 13–15 in Table 2) show the reproducibility of the results. Subsequently, the membrane ion removal percentage (Y) is predicted using the following equation:

$$Y = b_0 + \sum_{i=1}^{k} b_i X_i + \sum_{i<j=2}^{k} b_{ij} X_i X_j + \sum_{h<i<j=3}^{k} b_{hij} X_h X_i X_j + e \quad (2)$$

Table 2 | Matrix of effective variables/levels (the Box-Behnken design) and real ion removal

	Factors			
Exp. #	**pH**	**C_0 (ppm)**	**TMP (bar)**	**Ion Removal, *R* (%)**
1	2	20	2	32.0
2	5	20	2	39
3	2	200	2	11.5
4	5	200	2	24.0
5	2	110	1	25.1
6	5	110	1	24.4
7	2	110	3	13.0
8	5	110	3	20.0
9	3.5	20	1	45.0
10	3.5	200	1	36.0
11	3.5	20	3	24.0
12	3.5	200	3	13.5
13	3.5	110	2	9.0
14	3.5	110	2	7.1
15	3.5	110	2	13.1

For $k = 3$, an example of a special cubic model, the above summation is expanded as follows:

$$Y = b_0 + b_1X_1 + b_2X_2 + b_3X_3 + b_{12}X_1X_2 + b_{13}X_1X_3 + b_{23}X_2X_3 + b_{123}X_1X_2X_3 + e \quad (3)$$

where b_i, b_{ii}, and b_{hij} are constants of linear (1D), quadratic (2D), and cubic (3D) as well as parameters' interactive mutual effects, respectively. X_i and X_j are independent variables' values in predetermined levels. b_0, k, and e are coefficients of regression, the number of parameters investigated and optimized, and the predictive model random error. The pH, C_0, and TMP parameters were assessed using BBD based on RSM (Hossaini Zahed *et al.* 2019; Peng *et al.* 2020; Singh & Bhateria 2020).

The best-fitted model regression equation for metal ion removal is determined as Equation (4) in terms of the real effective factors values as below:

$$\begin{aligned} R(\%) = &+ 106.20 - 13.81\, pH - 0.46\, C_0 - 39.32\, TMP + 0.01\, pH \times C_0 \\ &+ 1.28\, pH \times TMP - 0.004\, C_0 \times TMP + 1.75\, (pH)^2 + 0.002\, C_0^2 \\ &+ 6.94\, (TMP)^2 \end{aligned} \quad (4)$$

Table 3 tabulates the variance results for the impacts of pH, C_0 and TMP as the independent factors and their interactions on Cu(II) ion removal.

The R^2 value for the fitted equation equals 0.9935, from which it can be found that the proposed model predicts the experimental data accurately. Table 3 also demonstrates that the pH factor's effect is less significant than the C_0 and TMP factors.

Actual experimental data for Cu(II) ion removal versus those predicted by the suggested model are revealed in Figure 4. From Figure 4, the model predicts the actual results well by the model, since the line drawn between the two sets of real and predicted data displays the angle of 45°.

Effects of single parameters on Cu(II) ion removal

Figure 5 demonstrates the effects of pH, C_0 and TMP on ion removal performance of the prepared membranes. The predicted results of the proposed model are presented in solid black lines, whereas the discrete blue lines show their confidence interval (CI, by 95%). The 95% CI is an interval estimate obtained from the statistical evaluation of the actual experimental data that might estimate the real values of indefinite factors.

Table 3 | The analysis of variance (ANOVA) parameters for the cubic model of ions removal

	Sum of Squares[a]	Degrees of Freedom[b]	Mean Square[c]	F Value[d]	*p*-value Prob > F[e]	Note[f]
Model	1,708.39	9	18.829	5.80	0.0337	Significant
A: pH	83.20	1	83.20	2.54	0.1718	
B: C_0	378.13	1	378.13	11.55	0.0193	Significant
C: TMP	450.00	1	450.00	13.74	0.0139	Significant
AB	7.56	1	7.56	0.2310	0.6511	
AC	14.82	1	14.82	0.4572	0.5309	
BC	0.5625	1	0.5625	0.0172	0.9008	
A^2	57.49	1	57.49	1.76	0.2425	
B^2	618.81	1	618.81	18.90	0.0074	Significant
C^2	178.13	1	178.13	5.44	0.0670	

[a]Sum of Squares: An index of how available data are dispersed around their mean and equals to the sum of squared differences between individual data and their mean (Sawyer 2009).

[b]Degrees of Freedom: Is a positive integer number obtained from the subtraction of the population parameters number from the independent observations count in a sample (Eisenhauer 2008).

[c]Mean Square is the average deviation of individual data from their mean and is equal to the sum of squares divided by their respective degrees of freedom (Sawyer 2009).

[d]F Value: is a ratio of statistical signal to the statistical noise in the system and calculated as the mean squares of data divided by data mean square into error mean square (Sawyer 2009).

[e]*p*-value Prob > F: as the p-value is less that confidence interval (here is 0.05), the respective model/variable is statistically significant (Sawyer 2009).

[f] Note: all the variable/models that have p-values less than confidence interval (here is 0.05) have determining impact on the dependent variable (i.e. Cu(II) ion removal) (Sawyer 2009).

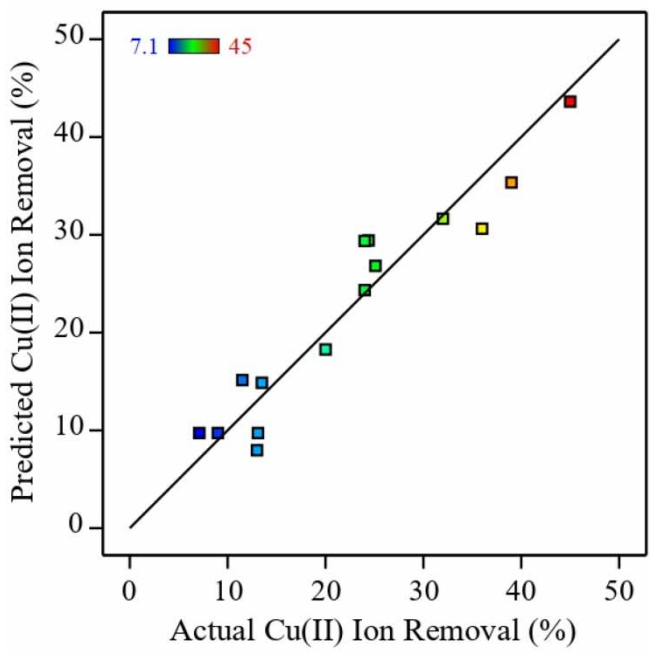

Figure 4 | Predicted versus actual values for Cu(II) ion removal.

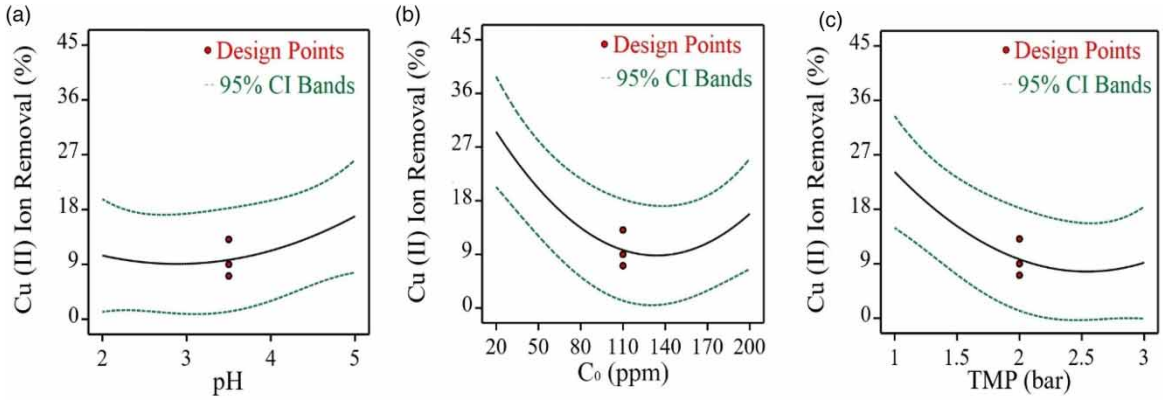

Figure 5 | Effect of feed solution: (a) effect of pH at TMP = 2 bar and C_0 = 110 ppm, (b) effect of initial feed concentration of Cu(II) ion at pH = 3.5 and TMP = 2 bar, and (c) effect of TMP at pH = 3.5 and C_0 = 110 ppm on ion removal performance (R, %) of the nanocomposite membrane loaded by 0.1 wt. % GNPs.

According to Figure 5(a), the ion removal trend increases slowly with the increase of pH from 2 to 5. In other words, Cu(II) ion removal decreases at acidic pH. Lower feed pH value eventuates at higher H^+ concentration; accordingly, this phenomenon accumulates protons on the membrane surface, which minimizes Cu(II) ion adsorptive removal by the membrane incorporated GNPs (Delavar *et al.* 2017). However, at pH values higher than 5, this trend becomes flat because of the $Cu(OH)_2$ formation, which significantly reduces Cu(II) ion removal (Sani *et al.* 2017).

Figure 5(b) shows that at ion concentration roughly below 140 ppm, ion removal increases as ion concentration decreases. In other words, the membrane shows the highest ion removal capacity at the lowest ion concentration. This is because GNPs' active adsorption sites can easily be adsorbed for Cu(II) ion adsorption in lower Cu(II) concentration conditions. Similar findings were published by Delavar *et al.* (2017). Beyond ion concentration of 140 ppm, a slight increase in the ion removal was observed; the reason for this phenomenon is not clear. Basically, a plateau graph is expected where more increase in C_0 results in no change in ion removal as observed. That means saturation occurs, and all active absorbent sites are occupied

with metal ions (Hafez 2012; Omri & Benzina 2012). Although more detailed studies are needed, and the clear and strong reason for this phenomenon is not available now, it was hypothesized that the slightly increasing trend in ion removal for ion concentration higher than 140 ppm may be related to the experimental error that alters the fitted equation.

Figure 5(c) shows that at TMPs up to 2.25 bar, ion removal decreases sharply. Higher TMP causes higher flux, which minimizes the probability of the copper divalent ion being taken by the membrane material. Therefore, its ion removal decreases. Beyond 2.25 bar, TMP hardly affects the Cu(II) ion removal. It is expected that by increasing the TMP the ion removal decreases in all the TMP range. This phenomenon was described as follows: Increasing the feed solution TMP increases the kinetic energy of the feed solution molecules, which can go through the pathway inside the membrane with a small pore size, which was not possible in low TMP. In this case, some part of the solution is treated with the NPs that were not in contact with any solution at low TMP, and fresh NPs inside the tiny pores well purify this part of the solution. Thus, the decreasing trend of the ion removal was damped by the above-mentioned phenomenon, and the removal plateaued above 2.25 bar.

Effect of selected dual parameters' interactions on ion removal

Figure 6 depicts 3D graphs of the selected dual parameters' interaction, in which two parameters are changed within their predetermined ranges selected in the BBD experimental design method, and the third one is kept constant at its middle value.

It can be seen in Figure 6(a) that the lowest membrane ion removal is reached when both TMP and C_0 gain their maximum levels; in other words, a simultaneous increase in TMP and C_0 reduces the membrane ion removal. Figure 6(b) shows that at any arbitrary C_0 in the selected range, the higher feed pH causes the higher ion removal, and at any arbitrary feed pH, ion removal is reduced as C_0 increases from 20 to 200 ppm. Figure 6(c) also shows that lower TMP results in higher ion removal regardless of feed pH; however, the minimum removal value is found at TMP of 2.25 bar and higher, as discussed before.

Optimum removal based on RSM optimization

As expected, the optimum conditions were selected by using the proposed RSM model to obtain the maximum of Cu(II) ion removal. Their values in this regard are 4.17 for pH, 20.291 ppm for C_0, and 1.009 bar for TMP, in which Cu(II) removal is 45.0%. A target pH (4.2), C_0 (20 ppm), and TMP (1 bar) were finally set regarding these proposed conditions in the experiment. The actual membrane performance was compared with that predicted by the proposed model at the same conditions in the experiments. The experimental results revealed 49.1% for removal of Cu(II) ion, which reveals an error of less than 9%. This shows a worthy agreement between the theoretically predicted value(s) and the experimentally measured actual result(s).

Lead removal

At the end, for the optimum condition of C_0 (20 ppm), pH (4.2) and TMP (1 bar) achieved from the Cu(II) ion removal optimization, the lead (Pb(II)) ion removal from synthetic wastewater was experimentally done. The result showed that 43% of the initial lead ions were removed, which is close to Cu(II) ions in the same filtration experiment conditions. The observed

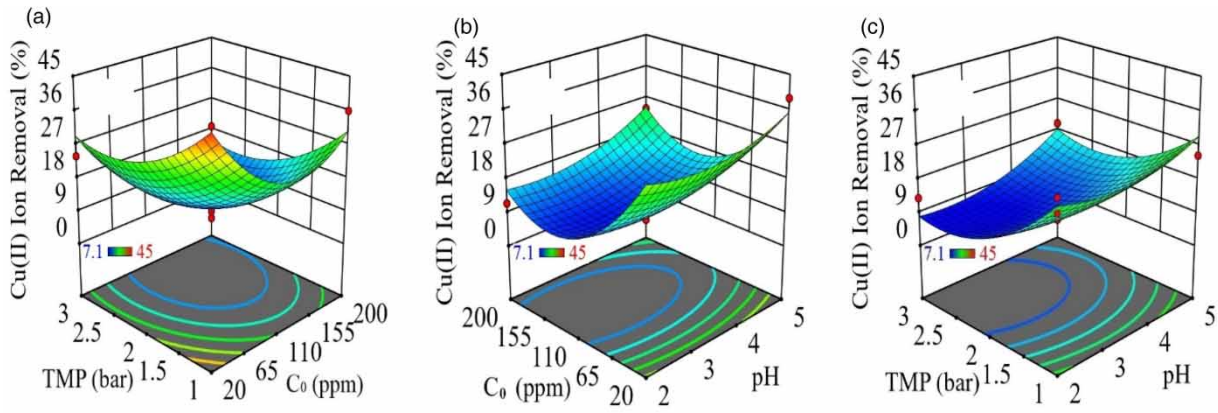

Figure 6 | Cu (II) ion removal surfaces as a function of (a) TMP and C_0 while pH is constant at 3.5; (b) C_0 and pH while TMP is constant at 2 bar; (c) TMP and pH while C_0 is constant at 110 ppm.

difference in the removal percentage may be due to the different ions of Cu(II) and Pb(II), as the former has a smaller diameter than the latter one. In other words, the larger ion occupies more space on the GNPs' adsorbent surface; hence, a lower number of ions are adsorbed, and a lower removal performance capacity is achievable. Besides the size of the ion, another effective parameter is hydration diameter, when ions are in aqueous solution and form aqua complexes in which the maximum number of water molecules are clustered around them. According to Persson (2010), both Cu(II) and Pb(II) form octahedrons with six water molecules forming the clusters around the metallic ion, with the larger hydrated ion radius for Pb(II) compared to Cu(II). Thus, the hydration diameter of Pb(II) is larger than that of Cu(II).

CONCLUSION

Previously prepared nanocomposite membranes based on PAN (15 wt. %)/PVP (1.3 wt. %) and the synthesized goethite nanoparticles (GNPs by 0.1 wt. %) via the phase separation method were used in the current study. The effects of pH, Cu(II) ion concentration, and transmembrane pressure on the Cu(II) ion removal were investigated. The obtained optimal conditions using BBD based on RSM was used to decide optimum conditions. Those at which the highest copper (Cu(II)) ion removal was achieved were 20 ppm for the feed ions concentration, 4.1 as the feed pH, and the operating TMP of 1 bar. According to the Box-Behnken experimental design, the predicted value for the membrane removal performance was 45%, which was reasonably close to 49.1%, the value obtained from the experiment. In addition, removal of lead (Pb(II)) metal ions was evaluated by the same membrane with the aforementioned initial feed conditions and operational TMP, and 43.0% ion removal was observed. Relatively low removal percent for Pb(II) ion can be attributed to the fact that the size-exclusion mechanism was not working due to the large pore size of the utilized ultrafiltration membrane, and adsorptive removal mechanism was employed mainly due to the incorporated GNPs' active site. Nasir *et al.* (2019) prepared PAN nanocomposite membranes incorporated with carbon nanotube and aluminium fumarate as adsorbent. Although they reached more than 90% Pb(II) removal, water permeability of their membrane was less than 8 LMH/bar (much less than that obtained in this research), which means their prepared membrane is located in the NF range. In another study, Pakdel Mojdehi *et al.* (2019), development of a polyethersulfone (PES) membrane modified by polyaniline TiO_2 adsorptive membrane was used for Cu(II) removal. In this study again, although near 90% Cu(II) ion removal was reported, water permeability was around 50 LMH/bar, much lower than that obtained for the membrane prepared in this study.

ACKNOWLEDGEMENT

The authors of this paper would like to acknowledge Iran National Science Foundation (INSF) for the financial support dedicated to the present research (Grant # 96008182).

DATA AVAILABILITY STATEMENT

All relevant data are included in the paper or its Supplementary Information.

REFERENCES

Bakoyannakis, D. N., Deliyanni, E. A., Zouboulis, A. I., Matis, K. A., Nalbandian, L. & Kehagias, T. 2003 Akaganeite and goethite-type nanocrystals: synthesis and characterization. *Microporous and Mesoporous Materials* **59** (1), 35–42.

Borbély, G. & Nagy, E. 2009 Removal of zinc and nickel ions by complexation–membrane filtration process from industrial wastewater. *Desalination* **240** (1), 218–226.

Cao, J., Tan, Y., Che, Y. & Xin, H. 2010 Novel complex gel beads composed of hydrolyzed polyacrylamide and chitosan: an effective adsorbent for the removal of heavy metal from aqueous solution. *Bioresource Technology* **101** (7), 2558–2561.

Charerntanyarak, L. 1999 Heavy metals removal by chemical coagulation and precipitation. *Water Science and Technology* **39** (10), 135–138.

Chatterjee, S. & De, S. 2014 Adsorptive removal of fluoride by activated alumina doped cellulose acetate phthalate (CAP) mixed matrix membrane. *Separation and Purification Technology* **125**, 223–238.

Choi, D. W. & Kim, Y. H. 2003 Cadmium removal using hollow fiber membrane with organic extradant. *Korean Journal of Chemical Engineering* **20** (4), 768–771.

Delavar, M., Bakeri, G. & Hosseini, M. 2017 Fabrication of polycarbonate mixed matrix membranes containing hydrous manganese oxide and alumina nanoparticles for heavy metal decontamination: characterization and comparative study. *Chemical Engineering Research and Design* **120**, 240–253.

Deliyanni, E. A., Kyzas, G. Z. & Matis, K. A. 2017 Various flotation techniques for metal ions removal. *Journal of Molecular Liquids* **225**, 260–264.

Eisenhauer, J. G. 2008 Degrees of freedom. *Teaching Statistics* **30** (3), 75–78.
Faur-Brasquet, C., Kadirvelu, K. & Le Cloirec, P. 2002 Removal of metal ions from aqueous solution by adsorption onto activated carbon cloths: adsorption competition with organic matter. *Carbon* **40** (13), 2387–2392.
Fazullin, D. D. & Mavrin, G. V. 2017 Effect of the pH of emulsion on ultrafiltration of oil products and nonionic surfactants. *Petroleum Chemistry* **57** (11), 969–973.
Fu, F. & Wang, Q. 2011 Removal of heavy metal ions from wastewaters: a review. *Journal of Environmental Management* **92** (3), 407–418.
Ghaemi, N. 2016 A new approach to copper ion removal from water by polymeric nanocomposite membrane embedded with γ-alumina nanoparticles. *Applied Surface Science* **364**, 221–228.
Hafez, H. 2012 A study on the use of nano/micro structured goethite and hematite as adsorbents for the removal of Cr(III), Co(II), Cu(II), Ni(II), and Zn(II) metal ions from aqueous solutions. *International Journal of Engineering Science and Technology* **4** (06), 3018–3028.
Hankins, N. P., Lu, N. & Hilal, N. 2006 Enhanced removal of heavy metal ions bound to humic acid by polyelectrolyte flocculation. *Separation and Purification Technology* **51** (1), 48–56.
Ho, J.-H., Yeh, Y.-N., Wang, H.-W., Khoo, S. K., Chen, Y.-H. & Chow, C.-F. 2014 Removal of nickel and silver ions using eggshells with membrane, eggshell membrane, and eggshells. *Food Science and Technology Research* **20** (2), 337–343.
Hossaini Zahed, S. S., Khanlari, S. & Mohammadi, T. 2019 Hydrous metal oxide incorporated polyacrylonitrile-based nanocomposite membranes for Cu(II) ions removal. *Separation and Purification Technology* **213**, 151–161.
Huang, J.-H., Shi, L.-J., Zeng, G.-M., Li, X., He, S.-B., Li, F., Xiong, Y.-L., Guo, S.-H., Zhang, D.-M. & Xie, G.-X. 2012 Effects of feed concentration and transmembrane pressure on membrane fouling in Cd^{2+} removal by micellar-enhanced ultrafiltration. *Desalination* **294**, 67–73.
Lalmi, A., Bouhidel, K.-E., Sahraoui, B. & Anfif, C. E. H. 2018 Removal of lead from polluted waters using ion exchange resin with $Ca(NO_3)_2$ for elution. *Hydrometallurgy* **178**, 287–293.
Mnif, A., Tabassi, D., Ben Sik Ali, M. & Hamrouni, B. 2015 Phenol removal from water by AG reverse osmosis membrane. *Environmental Progress & Sustainable Energy* **34** (4), 982–989.
Mulder, M. 1997 *Basic Principles of Membrane Technology*. Kluwer academic publisher, Boston, London.
Nasir, A. M., Goh, P. S., Abdullah, M. S., Ng, B. C. & Ismail, A. F. 2019 Adsorptive nanocomposite membranes for heavy metal remediation: recent progresses and challenges. *Chemosphere* **232**, 96–112.
Omri, A. & Benzina, M. 2012 Removal of manganese(II) ions from aqueous solutions by adsorption on activated carbon derived a new precursor: *Ziziphus spina-christi* seeds. *Alexandria Engineering Journal* **51** (4), 343–350.
Oo, M. H. & Song, L. 2009 Effect of pH and ionic strength on boron removal by RO membranes. *Desalination* **246** (1), 605–612.
Pakdel Mojdehi, A., Pourafshari Chenar, M., Namvar-Mahboub, M. & Eftekhari, M. 2019 Development of PES/polyaniline-modified TiO_2 adsorptive membrane for copper removal. *Colloids and Surfaces A: Physicochemical and Engineering Aspects* **583**, 123931.
Peng, X., Yang, G., Shi, Y., Zhou, Y., Zhang, M. & Li, S. 2020 Box–Behnken design based statistical modeling for the extraction and physicochemical properties of pectin from sunflower heads and the comparison with commercial low-methoxyl pectin. *Scientific Reports* **10** (1), 3595.
Persson, I. 2010 Hydrated metal ions in aqueous solution: how regular are their structures? *Pure and Applied Chemistry* **82** (10), 1901–1917.
Rahimi, S., Moattari, R. M., Rajabi, L., Derakhshan, A. A. & Keyhani, M. 2015 Iron oxide/hydroxide (α,γ-FeOOH) nanoparticles as high potential adsorbents for lead removal from polluted aquatic media. *Journal of Industrial and Engineering Chemistry* **23**, 33–43.
Saksena, S. & Zydney, A. L. 1994 Effect of solution pH and ionic strength on the separation of albumin from immunoglobulins (IgG) by selective filtration. *Biotechnology and Bioengineering* **43** (10), 960–968.
Sani, H. A., Ahmad, M. B., Hussein, M. Z., Ibrahim, N. A., Musa, A. & Saleh, T. A. 2017 Nanocomposite of ZnO with montmorillonite for removal of lead and copper ions from aqueous solutions. *Process Safety and Environmental Protection* **109**, 97–105.
Sawyer, S. F. 2009 Analysis of variance: the fundamental concepts. *Journal of Manual & Manipulative Therapy* **17** (2), 27E–38E.
Singh, R. & Bhateria, R. 2020 Optimization and experimental design of the Pb^{2+} adsorption process on a nano-Fe_3O_4-based adsorbent using the response surface methodology. *ACS Omega* **5** (43), 28305–28318.
Tofighy, M. A. & Mohammadi, T. 2011 Adsorption of divalent heavy metal ions from water using carbon nanotube sheets. *Journal of Hazardous Materials* **185** (1), 140–147.
Tran, T.-K., Leu, H.-J., Chiu, K.-F. & Lin, C.-Y. 2017 Electrochemical treatment of heavy metal-containing wastewater with the removal of COD and heavy metal ions. *Journal of the Chinese Chemical Society* **64** (5), 493–502.
Verbeken, K., Vanheule, B., Pinoy, L. & Verhaege, M. 2009 Cobalt removal from waste-water by means of supported liquid membranes. *Journal of Chemical Technology & Biotechnology* **84** (5), 711–715.
Yin, J. & Deng, B. 2015 Polymer-matrix nanocomposite membranes for water treatment. *Journal of Membrane Science* **479**, 256–275.
Yu, Y., Zhao, C., Wang, Y., Fan, W. & Luan, Z. 2013 Effects of ion concentration and natural organic matter on arsenic(V) removal by nanofiltration under different transmembrane pressures. *Journal of Environmental Sciences* **25** (2), 302–307.

First received 13 October 2021; accepted in revised form 10 January 2022. Available online 25 January 2022